A. Colagrossi, M. Lavagna
*Preliminary Results on the Dynamics of Large and Flexible Space Structures in Halo Orbits*
Acta Astronautica, Vol. 134, 2017, p. 355-367
doi:10.1016/j.actaastro.2017.02.020

IAC–16–C1.6.1

# PRELIMINARY RESULTS ON THE DYNAMICS OF LARGE AND FLEXIBLE SPACE STRUCTURES IN HALO ORBITS

**Andrea Colagrossi**
Ph.D. Candidate, Department of Aerospace Science and Technology, Politecnico di Milano, Milan, Italy, andrea.colagrossi@polimi.it.

**Michèle Lavagna**
Associate Professor, Department of Aerospace Science and Technology, Politecnico di Milano, Milan, Italy, michelle.lavagna@polimi.it.

The global exploration roadmap suggests, among other ambitious future space programmes, a possible manned outpost in lunar vicinity, to support surface operations and further astronaut training for longer and deeper space missions and transfers. In particular, a Lagrangian point orbit location - in the Earth- Moon system - is suggested for a manned cis-lunar infrastructure; proposal which opens an interesting field of study from the astrodynamics perspective. Literature offers a wide set of scientific research done on orbital dynamics under the Three-Body Problem modelling approach, while less of it includes the attitude dynamics modelling as well. However, whenever a large space structure (ISS-like) is considered, not only the coupled orbit-attitude dynamics should be modelled to run more accurate analyses, but the structural flexibility should be included too. The paper, starting from the well-known Circular Restricted Three-Body Problem formulation, presents some preliminary results obtained by adding a coupled orbit-attitude dynamical model and the effects due to the large structure flexibility. In addition, the most relevant perturbing phenomena, such as the Solar Radiation Pressure (SRP) and the fourth-body (Sun) gravity, are included in the model as well. A multi-body approach has been preferred to represent possible configurations of the large cis-lunar infrastructure: interconnected simple structural elements - such as beams, rods or lumped masses linked by springs - build up the space segment. To better investigate the relevance of the flexibility effects, the lumped parameters approach is compared with a distributed parameters semi-analytical technique. A sensitivity analysis of system dynamics, with respect to different configurations and mechanical properties of the extended structure, is also presented, in order to highlight drivers for the lunar outpost design. Furthermore, a case study for a large and flexible space structure in Halo orbits around one of the Earth-Moon collinear Lagrangian points, L1 or L2, is discussed to point out some relevant outcomes for the potential implementation of such a mission.

## I. INTRODUCTION

During the last decade of the twentieth century humanity posed the bases for prolonged human habitation in space. In fact, the International Space Station (ISS) program achieved marvellous objectives in Low-Earth orbit and allowed to better understand the effects of spaceflight on human body. In the meantime, robotic exploration of Solar System made huge leaps forward as well; many planets and numerous celestial objects were explored as never before. At present time, space exploration goals are increasingly ambitious and, in few years from now, manned and unmanned space missions will cooperate to bring mankind further and further away from its cradle. The path to follow has been already proposed by the International Space Exploration Group (ISECG) [1], and one of the milestones to achieve is the so called Evolvable Deep Space Habitat: a modular space station in lunar vicinity.

The configuration of the entire space station and its ideal orbit location still has to be determined, even though a favourable solution for the latter could be found among orbits that exist under the Three-Body Problem modelling approach. Actually, recent studies proposed different Keplerian and non-Keplerian options to operate a space system in cis-lunar space, and orbits that exist in the Circular Restricted Three Body Problem (CR3BP) seem the most promising ones [2]. For example, orbits about one of the Earth-Moon collinear libration points, such as EML (Earth-Moon Lagrangian Point) Halo orbits, have continuous line of sight coverage for communications and their Earth accessibility with existing transportation systems is good. However, also other CR3BP orbit types have appealing properties, such as the excellent orbit stability of Distant Retrograde Orbits (DRO) or the satisfactory ease of access from the Moon of Near-Rectilinear Orbits (NRO). In this paper, all the aforementioned families of orbits are considered and analysed, but greater attention is dedicated to

libration point Halo orbits, both with regular amplitude (Halo) or with large amplitude (NRO).

Most of the existing research done in this context is however founded on dynamical models based on point-mass dynamics, which is sometimes not sufficient to carry out accurate analysis when a large space system is considered. In fact, when the attitude dynamics is coupled with the orbital motion in a non-Keplerian environment, the rotational behaviour of the interested body may have extremely complex evolutions. Nevertheless, under the chaotic appearance that is typical when more than one massive body is considered, there could be regular dynamical structures that may be exploited to design space missions, leveraging the attitude dynamics to satisfy very complicated requirements. For example, naturally periodic orbit-attitude solutions could enable coarse pointing operational modes for data acquisition or communications without a relevant control action. Moreover, an important improvement in pointing accuracy or rendezvous and docking safety could be obtained knowing the natural attitude evolution of a spacecraft in complex dynamical environments. Alternatively, information on attitude instability can be used to design and drive large slewing manoeuvres.

An additional important aspect, which has rarely been considered studying the dynamics of a spacecraft in non-Keplerian orbits, is the influence between the space structure flexibility and the orbital and attitude dynamics. In fact, having in mind the structural properties of a ISS-like space structure, it is reasonable to investigate if it is possible to assume rigid body dynamics while modelling such a kind of large space systems. The information gathered from these analyses can be applied to highlight the validity range in assuming rigid body motion, to assess true closed loop stability or effective actuation of an attitude control systems designed for a large space structure in complex dynamical environments.

Therefore, there is a legitimized reason to better understand the coupled interactions between orbital, attitude and flexible dynamics in non-Keplerian dynamical environments, such as the CR3BP regime.

First investigations about attitude dynamics in the restricted three-body problem assumed the spacecraft as artificially maintained close to the equilibrium points and only the stability of the motion was considered [3, 4]. Afterwards, Euler parameters were introduced to study the rotational dynamics of a single body located at one of the Lagrangian point [5]. More recently, other authors focused their attention to the attitude dynamics of a spacecraft in the vicinity of equilibrium points, using Poincarè maps and linear approximations of non-Keplerian orbits [6, 7].

In the last few years, the coupling between orbital and attitude motion was investigated by Guzzetti considering planar motion and providing different families of orbit-attitude solutions [8, 9]. Additional studies conducted by Knutson explored the full three-dimensional coupled motion for a multi-body spacecraft in the Earth-Moon system [10, 11]. Both the two previous authors dedicated their research works to identify conditions that determine bounded attitude solutions relative to the CR3BP synodic frame in non-Keplerian reference trajectories.

Most recently, Colagrossi and other researchers at Politecnico di Milano developed different models to study fully coupled orbit-attitude motion in three-dimensional and planar space, with applications to various scientific and technological objectives [12, 13].

The paper starts presenting a fully coupled model for orbit-attitude dynamics, which is based on a Circular Restricted Three-Body Problem formulation. The equations of motion take also into account the most relevant perturbing phenomena, such as the Solar Radiation Pressure (SRP), the fourth-body (Sun) gravity and the variation in the gravitational attraction due to the finite dimension of the large space structure. Subsequently, a multiple shooting algorithm is described and it is used to find solutions that are periodic in both the orbital and attitude states. Moreover, a method to generate initial guesses for the numerical boundary value problem solver is presented.

The second part of the research analyses the interactions between orbit-attitude and flexible dynamics. A distributed parameters model, based on the Ritz method, is exploited to simulate the dynamics of a generic slender body undergoing large overall motions. Furthermore, a lumped parameters model has been developed and compared with the distributed parameters technique. The two approaches can be used together to assemble and simulate complex flexible space structures, because they are developed utilizing a multi-body formulation.

Lastly, representative solutions are illustrated and discussed, with particular attention to the case study of a large and flexible space structure in non-Keplerian orbits around one of the Earth-Moon collinear Lagrangian points.

## II. Orbit-Attitude Dynamical Model

The present orbit-attitude dynamical model is based on Circular Restricted Three-Body Problem modelling approach, which consider the motion of three masses $m_1, m_2$ and $m$, where $m \ll m_1, m_2$ and $m_2 < m_1$. $m_1$ and $m_2$ are denoted as primaries, and are assumed to be in circular orbits about their common centre of mass. The motion of $m$ does not affect the trajectories of the primaries.

The translational dynamics of $m$ is conveniently expressed in a rotating reference frame, $S$, which is called synodic frame and is shown in figure 1. It is centred at

the centre of mass of the system, $O$; the first axis, $\hat{\mathbf{x}}$, is aligned with the vector from $m_1$ to $m_2$; the third axis, $\hat{\mathbf{z}}$, is in the direction of the angular velocity of $S$, $\boldsymbol{\omega} = \omega\hat{\mathbf{z}}$; $\hat{\mathbf{y}}$ completes the right-handed triad. At time $t = 0$, the rotating frame $S$ is aligned to the inertial frame $I$, which is centred in $O$ and is defined by the axes $\hat{\mathbf{X}}$, $\hat{\mathbf{Y}}$ and $\hat{\mathbf{Z}}$.

The system can be defined by the mass parameter,

$$\mu = \frac{m_2}{m_1 + m_2},$$

the magnitude of the angular velocity of $S$,

$$\omega = \sqrt{\frac{G(m_1 + m_2)}{r_{12}^3}},$$

and the distance between the primaries $r_{12}$. The equations of motion are usually normalized such that $r_{12}$, $\omega$ and the total mass of the system, $m_T = m_1 + m_2$, are unitary in non-dimensional units. These units are indicated with the symbol $[\mathrm{nd}]$ in the paper. As a consequence, after the normalization, the universal constant of gravitation is $G = 1$ and the period of $m_1$ and $m_2$ in their orbits about their centre of mass is $T = 2\pi$. The location of $m_1$ along $\hat{\mathbf{x}}$ is $-\mu$, whereas $m_2$ is located at $1 - \mu$. In the Earth-Moon system the parameters to normalize the equations of motion are $r_{12} = 384\,400\,\mathrm{km}$, $m_T = 6.04 \times 10^{24}\,\mathrm{kg}$ and $T = 2\pi/\omega = 27.28\,\mathrm{d}$.

The body $m$ is extended, three-dimensional and, in this section, is assumed to be rigid. Hence, it has six degrees of freedom: the position of its centre of mass in $S$, which is easily described by the position vector $\mathbf{r}_B$, and the orientation of the body reference frame $B$ with respect to $I$ or $S$. To define the orientation of one frame with respect to another, three parameters are the minimal set required, but in this model the instantaneous orientation of $B$ is more conveniently described using the four-dimensional quaternion vector, also known as Euler parameters, as will be discussed in the following. The body-fixed frame $B$ is centred at the centre of mass of $m$, $O_B$, and it is aligned with the body principal inertia directions, $\hat{\mathbf{b}}_1$, $\hat{\mathbf{b}}_2$ and $\hat{\mathbf{b}}_3$.

The orbital dynamics of the body $m$ has been modelled considering the usual Circular Restricted Three-Body Problem formulation, valid for point-mass unperturbed dynamics, plus the contribution of the Solar Radiation Pressure, the fourth-body gravity and the variation in the gravitational attraction due to the finite dimension of $m$, expressed with the second order term of the force exerted on a finite dimension body by a particle.

The resulting problem is written in the following normalized scalar form:

$$\mathbf{f}_x = \begin{cases} \dot{x} = v_x \\ \dot{y} = v_x \\ \dot{z} = v_z \end{cases} \tag{1}$$

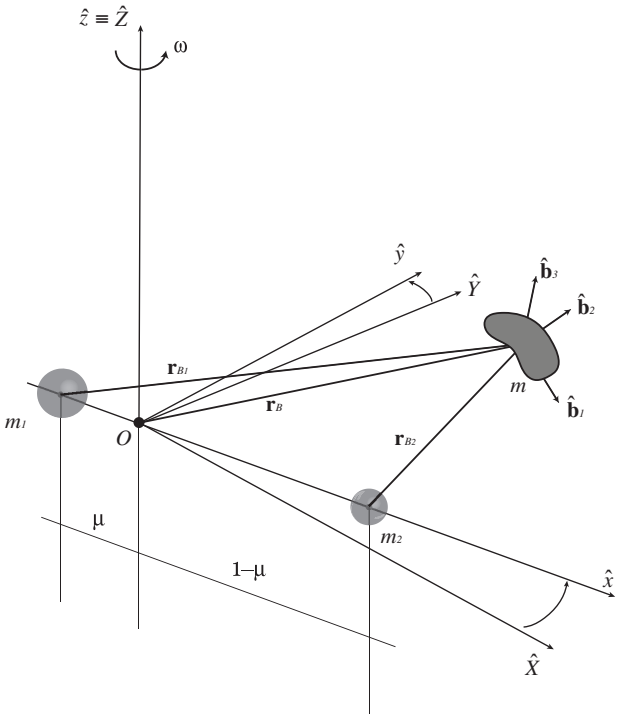


Fig. 1: Synodic and Inertial Reference Frames.

$$\mathbf{f}_v = \begin{cases} \dot{v}_x = x + 2v_y - \dfrac{(1-\mu)(x+\mu)}{r_{B_1}^3} - \dfrac{\mu(x-1+\mu)}{r_{B_2}^3} \\ \qquad\qquad + a_{SRP_x} + a_{4th_x} + a_{1_x} + a_{2_x} \\ \dot{v}_y = y - 2v_x - \dfrac{(1-\mu)y}{r_{B_1}^3} - \dfrac{\mu y}{r_{B_2}^3} \\ \qquad\qquad + a_{SRP_y} + a_{4th_y} + a_{1_y} + a_{2_y} \\ \dot{v}_z = -\dfrac{(1-\mu)z}{r_{B_1}^3} - \dfrac{\mu z}{r_{B_2}^3} \\ \qquad\qquad + a_{SRP_z} + a_{4th_z} + a_{1_z} + a_{2_z}, \end{cases} \tag{2}$$

where $x$, $y$ and $z$ are the Cartesian coordinates of $O_B$ expressed in terms of the synodic reference frame; $v_x$, $v_y$ and $v_z$ are the velocity components of the body $m$ in $S$. The distances between the centre of mass of $m$ and the two primaries are respectively $r_{B_1} = \sqrt{(x+\mu)^2 + y^2 + z^2}$ and $r_{B_2} = \sqrt{(x-1+\mu)^2 + y^2 + z^2}$, as can be easily noted from figure 1.

The variation in the gravitational attraction due to the finite dimension of the body, which is represented by the additional terms $a_{1_x}$, $a_{1_y}$ and $a_{1_z}$ for the first primary $m_1$, and by $a_{2_x}$, $a_{2_y}$ and $a_{2_z}$ for the second primary $m_2$, is due

to the fact that the resultant gravity force on a particle and on an extended body are different. When a large space structure is taken into account, the gravitational attraction is also dependent from the relative orientation of $m$ with respect to each primary. In fact, the force exerted on the extended body by the $i$-th primary can be computed as a series expansion:

$$\mathbf{\Gamma}_i = -\frac{Gmm_i}{r_{B_i}^2}\left(\hat{\mathbf{r}}_{B_i} + \sum_{j=2}^{\infty}\mathbf{G}_{j_i}\right), \tag{3}$$

where $\mathbf{G}_{j_i}$ is a collection of terms of $j$-th degree in $\rho/r_{B_i}$: $\rho$ is the distance of a generic point of $m$ with respect to the centre of mass, $O_B$, and $\hat{\mathbf{r}}_{B_i}$ is the unit vector directed from the $i$-th primary towards $O_B$. The series expansion in equation (3) is valid and converges for a body that is small compared to the distance from the primary, such that $\rho/r_{B_i} \ll 1$. Obviously, the first element in the bracket is the usual point-mass contribution and it is already included in the nominal CR3BP equations, which are written in the first rows of each right-hand side of equation (2). Therefore, the variation in the gravitational attraction due to the finite dimension of the body is determined by the summation of terms of $j$-th degree. In particular, limiting the expansion at the second degree, $\mathbf{G}_{2_i}$ is given by:

$$\mathbf{G}_{2_i} = \frac{1}{mr_{B_i}^2}\left\{\frac{3}{2}\left[\mathrm{tr}(\mathbf{I}) - 5\hat{\mathbf{r}}_{B_i}\cdot\mathbf{I}\cdot\hat{\mathbf{r}}_{B_i}\right]\hat{\mathbf{r}}_{B_i} + 3\mathbf{I}\cdot\hat{\mathbf{r}}_{B_i}\right\}, \tag{4}$$

where $\mathbf{I}$ is the body inertia tensor about the centre of mass [14]. This equation is computed at each integration step, knowing the position and the orientation of the body $m$ with respect to each primary. In particular, the attitude dynamics is needed to find the direction cosines of the body reference frame $B$ relative to a frame $A_i$, which has the first axis aligned as $\hat{\mathbf{r}}_{B_i}$ and the other two axes form a right-handed orthogonal coordinate frame: the second and third axis of $A_i$ are chosen to be mutually perpendicular and orthogonal to $\hat{\mathbf{r}}_{B_i}$ and to $\hat{\mathbf{z}}$. In general, $\mathbf{G}_{2_i}$ is not parallel to $\hat{\mathbf{r}}_{B_i}$ and the resultant gravity force does not align with the vector from the primary to the body centre of mass. The acceleration term that is representing this variation can be obtained from equation (4) and equation (3), normalized for the CR3BP formulation and inserted in equation (2) through $a_{1_{x,y,z}}$ and $a_{2_{x,y,z}}$, respectively valid for the first and the second primary. These terms are not particularly relevant for small bodies when compared to other perturbing phenomena, such as the SRP or the Sun's gravity. But, when the dynamics of a large space structure is investigated, they should be considered together with the additional perturbing terms to run accurate analyses. For example, for a ISS-like spacecraft orbiting around L1, their contribution is only 3 to 4 orders of magnitude smaller than the one determined by the other perturbations considered in this investigation.

The presence of the Sun is another important aspect that should be considered, especially when an accurate model to propagate the motion at a significant distance from any primary gravitational attractor is sought. In this model, the Sun is included both with its gravitational effect and its radiation contribution. In this regards, the model is maintained within the Earth-Moon synodic frame but the position of the Sun is computed in the inertial frame $I$, exploiting an ephemeris model contained in the SPICE Toolkit by NASA / JPL. For this purpose, the frame $I$ is centred in the Earth-Moon barycentre, $O$, as previously introduced, and it is assumed to be parallel to the Ecliptic J2000 reference. The latter assumption is quite valid also considering the definition of the synodic frame $S$; in fact, the orbital plane of the Moon is inclined to the ecliptic by only $5\mathrm{deg}$ and it is possible to choose $t = 0$ when the $\hat{\mathbf{x}}$-axis is almost aligned with the Vernal Equinox direction as seen from the Earth. Therefore, $S$ at $t = 0$, which is coincident with $I$, is approximately aligned to the Ecliptic J2000 reference used to compute the ephemerides. When the position of the Sun is known in $I$, it is straightforward to transform it in the synodic frame. Afterwards, the solar radiation pressure contribution and the fourth-body gravitational effect can be easily evaluated.

The solar radiation pressure is an expression for the interaction between incoming photons from the Sun and a surface that is invested by such a flux. The radiation can interact with a generic body by reflection or absorption, and since it carries momentum and energy, this interaction generates a pressure that perturbs the dynamics. The average pressure due to radiation can be computed using:

$$P_{SRP} = \frac{\Lambda_{SRP}}{c}, \tag{5}$$

where $c = 299\,792\,458\,\mathrm{m/s}$ is the speed of light, and $\Lambda_{SRP}$ is the flux density of solar radiation at the distance of the body from the Sun. It can be computed with an inverse square law, knowing the flux of solar radiation at a certain location in Space. For example, in the Earth-Moon system $\Lambda_{SRP} \simeq 1350\,\mathrm{w/m^2}$. The fraction of radiation associated that can be absorbed, specularly reflected and reflected with diffusion is expressed by a coefficient of absorption, $c_a$, diffuse reflection, $c_d$, and specular reflection, $c_r$. The coefficients must sum to unity, $c_a + c_d + c_r = 1$, and in this work they are assumed to have the typical values for the materials used in the space system. The force that is generated by the solar radiation pressure interaction can be computed using the expression for the radiation pressure on a flat surface; no approximation is made in addition to the one of discretizing the real body with a series of flat surfaces, and the self-shadowing effect can be taken

into account with simple geometrical considerations. For the $i$-th body planar surface of area $A_i$, the solar radiation force can be expressed as:

$$\mathbf{\Gamma}_{SRP_i} = -A_i P_{SRP} \Bigg[ (1 - c_r)\hat{\mathbf{s}} + 2 \left( c_r \cos(\alpha_i) + \frac{1}{3} c_d \right) \hat{\mathbf{n}}_i \Bigg] \cos(\alpha_i)_{Sh}, \quad (6)$$

where $\hat{\mathbf{s}}$ and $\hat{\mathbf{n}}_i$ are, respectively, the Body-Sun direction and the surface normal direction in the body-fixed frame. The angle $\alpha$ is the angle between the Body-Sun and the normal to the surface directions, and $\cos(\alpha)$ can only assume positive values since, if $\hat{\mathbf{n}}_i \cdot \hat{\mathbf{s}}$ is negative, the surface is in shadow and is not illuminated by the Sun. This can be mathematically expressed with $\cos(\alpha_i)_{Sh} = \max(0, \cos(\alpha_i))$. Equation (6) is obtained assuming that the absorbed radiation acts in the Body-Sun direction, the specularly reflected radiation acts in the normal to the surface direction and the diffuse radiation acts in both directions. The whole solar radiation force can be computed summing up equation (6) for each face that is included in the model. The resulting acceleration is normalized for the CR3BP formulation and inserted in equation (2) through $a_{SRP_{x,y,z}}$. Similarly, for what concern rotational motion, the solar radiation torque can be obtained knowing the centroid of each planar face and its position vector, $\mathbf{r}_{A_{i_B}}$, with respect to the centre of mass, $O_B$. In fact, the torque contribution of each face is directly computed as the moment produced by $\mathbf{\Gamma}_{SRP_i}$ about, $O_B$. The net solar radiation torque, $\mathbf{T}_{SRP}$, is the summation over all the planar faces and the related angular acceleration, $\boldsymbol{\alpha}_{SRP}$, is normalized and inserted in the attitude equations that will be discussed in the following.

The fourth-body gravitational effect is determined by the presence of the Sun, while the gravitational forces of all the other planets are neglected in this model. The dynamics of $m$ is influenced by the gravitational attraction of the two primaries, which are revolving in circular orbits around their centre of mass, as described by the first part of equation (2) written in the synodic frame. However, it is currently assumed that the whole Restricted Three-Body System is influenced by the gravity of the Sun and $O$ is revolving according to the Ephemeris model around the centre of mass of the Solar System. In order to simplify the description of the overall motion, the $S$ frame is used anyhow; when the position of the Sun is gathered from the ephemerides in $I$, it is subsequently rotated in $S$, where the Earth and Moon have fixed positions and the Sun is rotating clockwise around the barycentre of the Earth-Moon system. Note that the assumed motions do not satisfy Newton's equations but, since it is an enhanced version of the Bicircular Four-Body Model, previous works showed that, in some regions of phase space, this model gives the same qualitative behaviour as the real system [15]. The fourth-body gravitational force can be computed as:

$$\mathbf{\Gamma}_S = -Gmm_S \left( \frac{\hat{\mathbf{r}}_{B_S}}{r_{B_S}^2} - \frac{\hat{\mathbf{r}}_{O_S}}{r_{O_S}^2} \right), \quad (7)$$

where $m_S$ is the mass of the Sun, $\hat{\mathbf{r}}_{B_S}$ and $r_{B_S}$ are respectively direction and magnitude of the vector from the Sun to the centre of mass of the body, $O_B$, while $\hat{\mathbf{r}}_{O_S}$ and $r_{O_S}$ are those related with the vector from the Sun to the barycentre of the Earth-Moon system, $O$. The previous equation is composed by two terms: the first one models the effect of the Sun on the spacecraft, while the second one models the effect of the fourth-body on the Earth-Moon system. The latter is needed because the frame $I$ is not really inertial, having its origin at the barycentre of Earth and Moon. The acceleration on $m$ can be directly obtained from equation (7) and, after the normalization for the CR3BP formulation, it can be inserted in equation (2) through $a_{4th_{x,y,z}}$. Particular attention is paid to numerical difficulties that might arise in computing equation (7), as typically discussed in the fundamental astrodynamics literature. For what concern rotational dynamics, the gravitational effect of the Sun is not uniform and determines a gravity gradient torque on a non-symmetric body, which is also present if the gravitational influence of the two main primaries is considered, as will be explained in the following. The effect of the gravity gradient on the rotational dynamics of $m$ can be expressed in the body-fixed frame, $B$, as:

$$\mathbf{T}_S = \frac{3Gm_S}{r_{B_S}^3} \begin{pmatrix} (I_3 - I_2) c_{S_2} c_{S_3} \\ (I_1 - I_3) c_{S_1} c_{S_3} \\ (I_2 - I_1) c_{S_1} c_{S_2} \end{pmatrix}, \quad (8)$$

where $c_{S_1}$, $c_{S_2}$ and $c_{S_3}$ are the direction cosines of the Sun-Body direction, $\hat{\mathbf{r}}_{B_S}$, in principal inertia axes; and $I_1$, $I_2$ and $I_3$ are the principal moments of inertia of $m$. The resulting angular acceleration, $\boldsymbol{\alpha}_{4th}$, is inserted, after the normalization, in the attitude equations of motion that will be examined next.

The attitude dynamics of $m$ allows to represent the orientation of the body reference frame $B$ with respect to a different frame. In the present model, the equations of rotational motion are written in the inertial frame, $I$, and the orientation of $B$ with respect to $S$ is computed with a simple frame transformation. The quaternion vector is used as attitude parameter and is denoted as:

$$\mathbf{q} = [q_1, q_2, q_3, q_4]^{\mathrm{T}}, \quad (9)$$

The components of the quaternion vector must satisfy the constraint:

$$q_1^2 + q_2^2 + q_3^2 + q_4^2 = 1; \quad (10)$$

therefore, just the first three components, $[q_1, q_2, q_3]^{\mathrm{T}}$, which identify the Euler axis of rotation, have to be defined to have a complete set of initial conditions. The fourth component, $q_4$, which gives information about the Euler angle, is automatically defined by the constraint in equation (10). The sign ambiguity that exist when $q_4$ is obtained from the quaternion constraint can be solved giving an initial condition for the sign of $q_4$ and enforcing the sign continuity during the numerical integration. The attitude parameters relate two reference frame and in this paper they are indicated as ${}^{C}\bullet^{D}$, where $C$ and $D$ are two generic reference frames and $\bullet$ is a generic attitude parameter. For example, the notation ${}^{I}\mathbf{q}^{B}$ means that the quaternion relates the frame $B$ with respect to the frame $I$. Quaternions have been used as attitude parameters because they have no singularity condition and just three components are sufficient to define the attitude of $m$, thanks to equation (10). Moreover, only the analysis of the quaternion subspace allows to highlight certain features of the considered dynamical system, as will be discussed in the following.

The fundamental rules of attitude kinematics allow the propagation the rotational motion from the attitude dynamics. In fact, it is possible to evaluate the time rate of change of the quaternion vector from the body angular velocity as:

$$\mathbf{f}_q = \begin{cases} \dot{q}_1 = \frac{1}{2}(\omega_1 q_4 - \omega_2 q_3 + \omega_3 q_2) \\ \dot{q}_2 = \frac{1}{2}(\omega_1 q_3 + \omega_2 q_4 - \omega_3 q_1) \\ \dot{q}_3 = \frac{1}{2}(-\omega_1 q_2 + \omega_2 q_1 + \omega_3 q_4) \\ \dot{q}_4 = -\frac{1}{2}(\omega_1 q_1 + \omega_2 q_2 + \omega_3 q_3), \end{cases} \tag{11}$$

where $\omega_1$, $\omega_2$ and $\omega_3$ are components of the angular velocity of the body relative to $I$ and expressed in the body-fixed reference frame $B$, ${}^{I}\boldsymbol{\omega}^{B}$; $q_1$, $q_2$, $q_3$ and $q_4$ are the quaternion components of ${}^{I}\mathbf{q}^{B}$. The angular velocity can be obtained integrating the equations for the rotational dynamics: the Euler equations of motion.

Euler equations includes the gravity torques exerted by the two primaries, which can be computed similarly to what has been done for the fourth body in equation (8). Moreover, the angular accelerations due to the Solar Radiation Pressure and to the gravity gradient of the fourth-body, Sun, are included in the model. They are obtained from the related torques described before and normalized for the CR3BP formulation. The resulting Euler dynamical equations for the attitude dynamics are expressed as:

$$\mathbf{f}_\omega = \begin{cases} \dot{\omega}_1 = \frac{I_3 - I_2}{I_1}\left(\frac{3(1-\mu)}{r_{B_1}^5} l_2 l_3 + \frac{3\mu}{r_{B_2}^5} h_2 h_3 - \omega_2\omega_3\right) + \alpha_{SRP_1} + \alpha_{4th_1} \\ \dot{\omega}_2 = \frac{I_1 - I_3}{I_2}\left(\frac{3(1-\mu)}{r_{B_1}^5} l_1 l_3 + \frac{3\mu}{r_{B_2}^5} h_1 h_3 - \omega_1\omega_3\right) + \alpha_{SRP_2} + \alpha_{4th_2} \\ \dot{\omega}_3 = \frac{I_2 - I_1}{I_3}\left(\frac{3(1-\mu)}{r_{B_1}^5} l_1 l_2 + \frac{3\mu}{r_{B_2}^5} h_1 h_2 - \omega_1\omega_2\right) + \alpha_{SRP_3} + \alpha_{4th_3}, \end{cases} \tag{12}$$

where $l_i$ are the direction cosines in the reference $B$ of the unit position vector from $m_1$ to $m$, $\hat{\mathbf{r}}_{B_1}$; $h_i$ are those related with $\hat{\mathbf{r}}_{B_2}$; $\alpha_{SRP_{1,2,3}}$ and $\alpha_{4th_{1,2,3}}$ are the components of the angular accelerations introduced before, respectively due to the SRP and to the presence of the Sun.

The contribution of solar radiation torque and fourth-body gravity gradient torque is in general few orders of magnitude smaller than the gravity gradient torques generated by the two primaries. However, their effect should not be neglected to run accurate simulations, especially when dealing with large space structures in lunar vicinity. For example, in a typical L1 orbit, the Earth and the Moon generate a gravity gradient torque respectively in the order of $10^{-4}$ Nm and $10^{-3}$ Nm, while the fourth-body effect is around $10^{-6}$ Nm. For what concern the solar radiation pressure, the magnitude of the torque depends also on the dimensions and the geometry of the spacecraft itself, but for a ISS-like structure the magnitude of this perturbing term is also in the order of $10^{-6}$ Nm.

Equations (1), (2), (11) and (12) complete the whole set of coupled equations of motion that is needed to describe the orbit-attitude dynamics of a rigid body in a Circular Restricted Three-Body Problem environment plus the presence of the gravitational attraction from the Sun and the Solar Radiation Pressure. Moreover, including the second order term of the force exerted on the finite dimension body by a point-mass, the model is not limited to small rigid bodies and it can be applied to any kind of spacecraft in the Earth-Moon system. The complete set of non-linear differential equations will be denoted as $\mathbf{f} = \{\mathbf{f}_x, \mathbf{f}_v, \mathbf{f}_q, \mathbf{f}_\omega\}$.

## III. Orbit-Attitude Periodic Motion

The equations of motion presented in the previous section do not have an analytical solution space, as it is generally true for the dynamics propagated in a CR3BP environment. Therefore, equations (1), (2), (11) and (12) have to be numerically integrated to analyse the motion evolution of $m$. However, the solutions are extremely sensitive to the set of initial conditions and a numerical targeting algorithm is needed, if one wants to highlight a particular behaviour or obtain a certain final condition. A very common method to find specific solutions in non-Keplerian environments is employed in this research, following the idea introduced in the last decades of the twentieth century and presented also in the work of Guzzetti [8]. In fact, a multiple shooting scheme, together with a multi-variable Newton-Raphson solver, is exploited to find orbit-attitude periodic solutions.

The idea of this numerical method is founded on the possibility to propagate the dynamics in the vicinity of reference solution. In fact, considering a generic non-linear set of equations of motion and a reference solution, $\bar{\mathbf{x}}$, it is possible to perturb the reference initial state vector, $\bar{\mathbf{x}}_0$, by a small quantity, $\delta\mathbf{x}_0$. Then, the linear evaluation for the behaviour of the variation, $\delta\mathbf{x} = \mathbf{x}(\bar{\mathbf{x}}_0 + \delta\mathbf{x}_0, t) - \bar{\mathbf{x}}(\bar{\mathbf{x}}_0, t)$, relative to the reference motion can be obtained using the Jacobian of the original non-linear system, $J(t) = \frac{\partial \mathbf{f}}{\partial \mathbf{x}}$, where the state vector is composed by: $\mathbf{x} = [x; y; z; v_x; v_y; v_z; q_1; q_2; q_3; w_1; w_2; w_3]$. Note that only three components of the quaternion have to be defined to completely define the system $\mathbf{f}$. In fact, the first-order variational equation can be written as:

$$\delta\dot{\mathbf{x}} = J(t)\delta\mathbf{x}. \tag{13}$$

At this point, the effect of variations in the initial state on $\delta\mathbf{x}$ can expressed in a linear sense as:

$$\delta\mathbf{x} = \left(\frac{\partial \mathbf{x}}{\partial \mathbf{x}_0}\right)\delta\mathbf{x}_0. \tag{14}$$

The linear differential relationship between initial and final state, $\frac{\partial \mathbf{x}}{\partial \mathbf{x}_0}$, which is known as State Transition Matrix (STM) and is denoted as $\Phi(t, t_0)$, can be related to a first-order differential equation governing its evolution. In fact, from equations (13) and (14) after some manipulations, it is possible to write:

$$\dot{\Phi}(t, t_0) = J(t)\Phi(t, t_0), \tag{15}$$

where the elements of the matrix $\Phi(t, t_0)$ represent the partial derivatives of the state, $\mathbf{x}$, at time $t$ with respect to the initial state, $\mathbf{x}_0$, at time $t_0$ that are integrated simultaneously with the equations of motion to produce the STM at any time along the integrated trajectory relative to a reference solution. Obviously, a variation in the initial state vector can only influence itself if the equations are not integrated and just evaluated at $t = t_0$. Hence, the initial condition for the STM in equation (15), is the identity matrix:

$$\Phi(t_0, t_0) = \mathcal{I}. \tag{16}$$

In order to integrate equation (15), the time-variant Jacobian of the system must be computed. It contains the partial derivatives of the system $\mathbf{f}$ with respect to the state vector $\mathbf{x}$:

$$J(t) = \begin{bmatrix} \frac{\partial \mathbf{f}_x}{\partial \mathbf{x}_B} & \frac{\partial \mathbf{f}_x}{\partial \mathbf{v}_B} & \frac{\partial \mathbf{f}_x}{\partial {}^I\mathbf{q}_B^B} & \frac{\partial \mathbf{f}_x}{\partial {}^I\boldsymbol{\omega}_B^B} \\ \frac{\partial \mathbf{f}_v}{\partial \mathbf{x}_B} & \frac{\partial \mathbf{f}_v}{\partial \mathbf{v}_B} & \frac{\partial \mathbf{f}_v}{\partial {}^I\mathbf{q}_B^B} & \frac{\partial \mathbf{f}_v}{\partial {}^I\boldsymbol{\omega}_B^B} \\ \frac{\partial \mathbf{f}_q}{\partial \mathbf{x}_B} & \frac{\partial \mathbf{f}_q}{\partial \mathbf{v}_B} & \frac{\partial \mathbf{f}_q}{\partial {}^I\mathbf{q}_B^B} & \frac{\partial \mathbf{f}_q}{\partial {}^I\boldsymbol{\omega}_B^B} \\ \frac{\partial \mathbf{f}_\omega}{\partial \mathbf{x}_B} & \frac{\partial \mathbf{f}_\omega}{\partial \mathbf{v}_B} & \frac{\partial \mathbf{f}_\omega}{\partial {}^I\mathbf{q}_B^B} & \frac{\partial \mathbf{f}_\omega}{\partial {}^I\boldsymbol{\omega}_B^B} \end{bmatrix}, \tag{17}$$

where $\mathbf{x}_B$, $\mathbf{v}_B$, ${}^I\mathbf{q}_B^B$ and ${}^I\boldsymbol{\omega}_B^B$ are the elements of the state vector $\mathbf{x}$, respectively related with the orbital position, the orbital velocity, the attitude parameters and the angular velocity of the body $m$. It must be noted that for the coupled orbit-attitude dynamics without perturbations $\frac{\partial \mathbf{f}_x}{\partial \mathbf{x}_B}$, $\frac{\partial \mathbf{f}_x}{\partial {}^I\mathbf{q}_B^B}$, $\frac{\partial \mathbf{f}_x}{\partial {}^I\boldsymbol{\omega}_B^B}$, $\frac{\partial \mathbf{f}_v}{\partial {}^I\mathbf{q}_B^B}$, $\frac{\partial \mathbf{f}_v}{\partial {}^I\boldsymbol{\omega}_B^B}$, $\frac{\partial \mathbf{f}_q}{\partial \mathbf{x}_B}$, $\frac{\partial \mathbf{f}_q}{\partial \mathbf{v}_B}$ and $\frac{\partial \mathbf{f}_\omega}{\partial \mathbf{v}_B}$ are equal to null matrices. However, when the previously introduced perturbations are included, the orbital motion is directly influenced by the orientation of the body and the partial $\frac{\partial \mathbf{f}_v}{\partial {}^I\mathbf{q}_B^B}$ is not equal to zero anymore.

The coupled orbit-attitude motion is described by 13 equations of motion contained in the system $\mathbf{f}$. Still, having in mind the constraint equation (10), only 12 equations are actually independent, because one of the kinematic relations in equation (11) is not necessary to completely describe the dynamics of the system: the fourth component of the quaternion vector can be derived from the Euler parameters constraint. Anyway, the modification of the system of differential equations $\mathbf{f}$ is not practical and it is maintained as described before, but the Jacobian and the STM are reduced to a 12 by 12 matrix, relating only the independent variables. This is done expressing the partials of the Jacobian relative to the quaternions as:

$$\frac{\mathrm{d}\mathbf{f}_i}{\mathrm{d}q_j}(q_1, q_2, q_3, q_4(q_1, q_2, q_3)) = \frac{\partial \mathbf{f}_i}{\partial q_j} - \frac{q_j}{q_4}\frac{\partial \mathbf{f}_i}{\partial q_4}, \tag{18}$$

which can be derived from the variational expression of equation (10). Therefore, considering the 13 equations of motion and the $12 \times 12$ linear differential relationships between initial and final state, there are 157 differential equations to be integrated in order to find orbit-attitude periodic solutions.

The Jacobian in equation (17) has been derived analytically for the coupled orbit-attitude dynamics without perturbations. The analytical expression of the partials has been obtained also for the variation in the gravitational attraction due to the finite dimension of the body. The effort in deriving such analytical expressions is justified by a relevant reduction in the computational cost of the algorithms that exploits that matrix. The terms in the Jacobian due to the Solar Radiation Pressure and the Sun gravity are instead computed numerically, since the presented model uses the ephemeris position of the Sun. In practice, when the terms related with the presence of the Sun are included, the State Transition Matrix is numerically obtained applying a small perturbation with respect to a reference initial condition, then the finite difference between the reference and the perturbed final state is available and the terms in the matrix can be numerically computed. This operation is done for each partial and the complete STM is finally assembled, even though it is not the real State Transition Matrix but just a numerical approximation. To assess the accuracy of this numerical STM, the result is continuously matched with the analytical STM without perturbations. A completely analytical Jacobian and State Transition Matrix with perturbations could be possible, without too much complexity, reducing the fidelity of the model for the position of the Sun, for example employing the original Bicircular Four-Body system.

With the availability of the State Transition Matrix, an algorithm able to find periodic solutions in both the orbital and attitude state can be implemented. In fact, it is possible to obtain a periodic motion in the rotating reference frame by iteratively correcting a reference path, but a good initial guess is needed. In this work, the targeting scheme is based on a multiple shooting strategy, which is very common in modern astrodynamics for the computation of periodic orbits. The idea is to find a solution that is continuous between the final and initial states in both the translational and rotational components, which is a typical two-point boundary value problem. However, the presented approach solves many Initial Value Problems where the different initial states are iteratively corrected, with a Newton approach, until the constraints at given patch points are satisfied, within a certain tolerance. In practice, the trajectory is discretized in $N$ patch points, which are associated with $N-1$ arcs. In the orbit-attitude coupled problem, each $i$-th patch point is the 12-dimensional state vector, $\mathbf{x}_i = [\mathbf{x}_{B_i}; \mathbf{v}_{B_i}; {}^I\mathbf{q}^B_{B_i}; {}^I\boldsymbol{\omega}^B_{B_i}]$. The first and last patch points are respectively the initial and final conditions. Each arc has the same time of flight, $T_a$, and therefore the complete solution has time of flight $T_t = (N-1)T_a$.

The problem has a free variables vector that includes the state vector in each patch point, plus the time of flight of a single arc:

$$\boldsymbol{\nu} = [\mathbf{x}_1; \ldots; \mathbf{x}_i; \ldots; \mathbf{x}_N; T_a]. \tag{19}$$

Hence the dimension of the problem is $n = 12N + 1$ and the free variables vector has to be corrected to satisfy a set of $m$ given constraints, collected in the vector $\boldsymbol{\mu}$. The periodic solution is identified as a set of $\bar{\boldsymbol{\nu}}$ that satisfies the constraint equations:

$$\boldsymbol{\mu}(\bar{\boldsymbol{\nu}}) = [\mu_1(\bar{\boldsymbol{\nu}}); \ldots; \mu_m(\bar{\boldsymbol{\nu}})] = \mathbf{0}. \tag{20}$$

This is done expanding the constraint function $\boldsymbol{\mu}$ about an initial guess $\boldsymbol{\nu}_0$ in a Taylor series to the first order:

$$\boldsymbol{\mu}(\boldsymbol{\nu}) \simeq \boldsymbol{\mu}(\boldsymbol{\nu}_0) + J_\mu(\boldsymbol{\nu}_0)(\boldsymbol{\nu} - \boldsymbol{\nu}_0), \tag{21}$$

where $J_\mu$ is the Jacobian of the constraint function with respect to the free variables $\nu$. Equation (21) is set equal to zero and iteratively solved for $\bar{\boldsymbol{\nu}}$.

Usually there are more free variables than constraint equations and so a minimum norm solution is exploited to produce the updated free variables vector. In fact, at the $k$-th iteration, the new solution is found as:

$$\boldsymbol{\nu}_{k+1} = \boldsymbol{\nu}_k - J_\mu(\boldsymbol{\nu}_k)^{\mathrm{T}} \left[J_\mu(\boldsymbol{\nu}_k) J_\mu(\boldsymbol{\nu}_k)^{\mathrm{T}}\right]^{-1} \boldsymbol{\mu}(\boldsymbol{\nu_k}). \tag{22}$$

This equation is recursively applied to update the free variables vector. When the equation (20) is solved within a certain numerical tolerance, the algorithm is stopped and the current solution $\boldsymbol{\nu}_k$ is the desired periodic solution $\bar{\boldsymbol{\nu}}$.

In this research, the constraint vector $\boldsymbol{\mu}$ is strongly related with the desired coupled orbit-attitude behaviour. The multiple shooting algorithm iteratively finds a solution that is periodic in both attitude and orbital state, has internal continuity at patch points between the different arcs and is sufficiently close to the desired initial guess. The periodicity is sought in the rotating synodic reference, but note that the attitude dynamics is expressed in the inertial frame. Hence, the quaternion ${}^I\mathbf{q}^B$ has to be transformed in the synodic reference, ${}^S\mathbf{q}^B$, prior to enforce periodicity. There is no need to transform the angular velocity of the body $m$ in the synodic reference, because the difference between the angular velocity measured in the inertial frame and in the rotating one is just a constant offset, which is not an issue for what concern periodicity: the periodicity constraints for the angular velocity can be expressed in both rotating and inertial frames. The orbital states do not need any addition modification since they are already expressed in $S$. Moreover, only 5 translational states have to be periodic; the remaining one is implicitly continuous because of the existence of an integral of motion, which is known as Jacobi constant. The presented coupled orbit-attitude dynamical model preserves this constant and the whole

algorithm is continuously assessed checking its value. One additional constraint is needed to fix a coordinate in the trajectory and phase all the orbits of a given family. Therefore, the constraint vector which is used in the algorithm is:

$$\boldsymbol{\mu}(\boldsymbol{\nu}) = \begin{bmatrix} (\mathbf{x}_1)_{T_a} - \mathbf{x}_2 \\ \vdots \\ (\mathbf{x}_{N-1})_{T_a} - \mathbf{x}_N \\ \\ x_N - x_1 \\ z_N - z_1 \\ v_{x_N} - v_{x_1} \\ v_{y_N} - v_{y_1} \\ v_{z_N} - v_{z_1} \\ \\ y_1 \\ \\ {}^S\mathbf{q}^B_{B_N} - {}^S\mathbf{q}^B_{B_1} \\ \\ {}^I\boldsymbol{\omega}^B_{B_N} - {}^I\boldsymbol{\omega}^B_{B_1} \end{bmatrix}, \tag{23}$$

where the continuity at patch points, the periodicity of 5 orbital states, the phasing of the family and the periodicity of attitude states are respectively listed. The result is a total of $m = 12N$ constraint equations composing the vector $\boldsymbol{\mu}$, which has to be nulled to find a periodic orbit-attitude solution.

A single periodic solution can be used to generate a dynamical family of other periodic solutions. The continuation process needs a separate initial guess, which can be obtained just modifying one parameter to the existing periodic solution or expanding in the direction of the null space of the State Transition Matrix computed over one orbital period of the reference solution (Monodromy Matrix). The latter is a well-known continuation scheme that is called pseudo-arclength continuation and is used in this investigation.

The search for periodic solutions needs an initial guess that is sufficiently close to the desired motion. Existing literature presents several methods able to provide approximation of the desired coupled dynamics, but many of them tries to find the geometry of the spacecraft that makes periodic a certain set of initial conditions. In this research a different method has been developed: starting from a given mass distribution of the body and, therefore, fixing its inertia parameters, the initial guess is generated with two distinct global optimization techniques, which are applied one after the other. In this way, it is possible to find a certain periodic orbit-attitude solution for a given mass distribution, instead of studying which is the body that can have a periodic motion on given orbit-attitude dynamics. Moreover, this method is faster and less demanding in computational resources than a standard search of periodic behaviours in a Poincarè map. The mass distribution of the body can be mathematically defined from the moments of inertia of the spacecraft or a combination of them, as will be explained afterwards.

The developed method begins with the definition of the inertia properties of the body, then the family and the period of the non-Keplerian orbit is introduced to identify the initial conditions for periodic orbital dynamics. At this point, the algorithm asks for the angular rate and the initial orientation of the attitude dynamics; these values do not have to generate a periodic motion, but they bind the inspection in a certain region of the attitude subspace. This step is fundamental to drive the algorithm in the desired direction and a bit of knowledge of the considered dynamical environment is necessary in order to have a fast convergence of the method. Next, the search for the initial guess is started, first with a genetic algorithm that optimizes the orbit-attitude initial conditions, then a pattern search algorithm refines the output of the genetic optimization. The goal of the two optimization techniques is to reduce the sum of the difference in all the orbit-attitude states, $\mathbf{x}$, at the starting point and after one period: periodicity error. The search for the initial guess is stopped when the periodicity error is below a given tolerance, which is low enough to allow the convergence of the multiple shooting Newton-Raphson solver.

The variables of the genetic algorithm are the 6 initial attitude states, while the initial orbital states are fixed and related to a given periodic orbit. The population is composed by 150 individuals, and it is initially generated with uniform distribution around a given initial guess. This user defined starting point, together with the bounds for the variables, confines the search space within the attitude subspace. Between two consecutive generations 5 best individuals are maintained and the crossover fraction of the remaining individuals is $70\%$. The maximum number of allowed generations is 175 and the stopping criteria are met when the periodicity error goes below $5 \times 10^{-2}\,\mathrm{nd}$. Then, a pattern search algorithm is started from the best solution found by the genetic algorithm, which has only to be refined. In fact, the tolerances for the search are very tight and the feasible poll points remains in the vicinity of the output of the previous optimization step. This further optimization step usually reduces the periodicity error between $1 \times 10^{-2}\,\mathrm{nd}$ and $1 \times 10^{-3}\,\mathrm{nd}$, allowing a very fast convergence of the multiple shooting algorithm. On a $2.5\,\mathrm{GHz}$ quad core processor that runs the optimization algorithms in parallel, the initial guess is usually found in about $20\,\mathrm{s}$, if good starting point and bounds are provided. The search needs few minutes in the worst conditions, which are caused by highly sensitive orbital families (e.g. NRO) and random starting point without bounds. Then,

on the same processor, the multiple shooting algorithm usually runs in about $10\,\mathrm{s}$ to reduce the periodicity error down to $1 \times 10^{-10}\,\mathrm{nd}$.

The developed method is based on global optimization techniques to search for an initial guess with heuristic strategies. The focus has not been directed on a particular optimization technique and the genetic algorithm has just proven to work well. No comparison with other heuristic optimization techniques has been carried out. In the same way, the refinement step accomplished by the pattern search method has just resulted in a faster convergence of the Newton-Raphson correction scheme. Further investigations might be of interest to compare different optimization methods in order to find the best ones in terms of computational speed and quality of the initial guess.

In figure 2 an initial guess is confronted with the relative periodic orbit-attitude solution for an example Halo orbit. From the picture, it is possible to understand that the initial guess solution must be very close to the periodic one, in order to have a good and fast convergence of the algorithm. Moreover, focusing on the coupled orbit-attitude periodic dynamics, it is evident that the passage close to the Moon generates a relevant angular acceleration, which is obviously due to the intense gravity gradient action exerted by the second primary on the body $m$. The orbit reported in figure 2a is a L1 Halo with period of $10.5\,\mathrm{d}$; the distribution of mass for $m$ is the one of a disk-like body with ratio between the maximum moment of inertia ($I_{max}$) and the minimum one ($I_{min}$) equal to 1.5. The initial conditions for the genetic algorithm are set to find an initial guess close to a simple spin dynamics around the body axis $\hat{\mathbf{b}}_3$, with the body reference frame and the inertial frame aligned at $t = 0$. The obtained initial guess is shown in figures 2a, 2c and 2e, while the periodic solution, output of the multiple shooting Newton-Raphson correction algorithm, is reported in figures 2b, 2d and 2f. The quaternions are shown as computed in the rotating synodic reference and, in order to simplify the notation, the quaternion ${}^{S}\mathbf{q}^{B}$ has been denoted as $\mathbf{q}_r$ in the plots. From figure 2d, it is possible to see that in the reported dynamics, the body $m$ is just librating and performs no overall rotation in $S$. The results shown in figure 2 have been obtained without the additional perturbing terms in the dynamical model. In table 1 the numerical values of the quaternion shown in figure 2d are reported for $t = 0$, $t = T_t/2$ and $t = T_t$, in order to accurately asses the periodicity of the solution and the fulfilment of the constraint equation (10).

Many other periodic solutions, for any kind of planar and spatial family of orbits in the CR3BP, were generated exploiting the presented multiple-shooting algorithm applied to the coupled orbit-attitude model. An example periodic solution is shown in figure 3 for a Near-Rectilinear Orbit. In this case, the period of the orbit is around $8.5\,\mathrm{d}$ and the mass distribution is the same that has been used to generate the Halo of figure 2. This case is particularly representative for all the NRO, since it shows the huge angular acceleration that exists during the passage very close to the Moon. Here, the gravity gradient influence of the second primary, already noted for the Halo periodic solution, is extremely emphasized and determines this typical behaviour for NRO. This aspect will be also discussed in a following section, but now is already possible to highlight that such an attitude evolution may pose problems for the structural integrity of a spacecraft orbiting in this class of orbits; a real extended space structure may experience difficulties in bearing the abrupt angular velocity variation shown in figure 3c. However, the large angular acceleration due to the Moon may be also effectively exploited to drive and facilitate large attitude slewing manoeuvres.

Table 1: Numerical Values of Periodic Orbit-Attitude Dynamics Quaternions (cf. figure 2d).

| | $\mathbf{q}_r$ |
|---|---|
| $t = 0$ | $[+0.000197, -0.020475, -0.009622, +0.999744]$ |
| $t = T_t/2$ | $[-0.000797, +0.061167, -0.009594, +0.998081]$ |
| $t = T_t$ | $[+0.000197, -0.020475, -0.009622, +0.999744]$ |

Figure 4 shows different periodic orbit-attitude dynamics in L1 Lyapunov Orbits, which were found to be remarkably sensitive to out-of-plane perturbations. In fact, the perturbations due to the Sun have been neglected and the orbit-attitude motion has been constrained on the $x$-$y$ plane. Additional investigations for Sun-perturbed Lyapunov orbits, within the employed ephemeris model, will have to be carried out, but an orbit control action may be necessary. However, the presented naturally periodic solutions reports three dissimilar rotational motions for a disk-like spacecraft, with moment of inertia ratio equal to 5. They are related to Lyapunov Orbits with period equal to $12.1\,\mathrm{d}$, $14.1\,\mathrm{d}$ and $18.88\,\mathrm{d}$. The attitude dynamics analysed in the quaternion subspace allows to point out and uniquely characterize the various dynamical families, which have different behaviours according to the orbital period and, therefore, the energy of the orbit. These results can be explained, as already highlighted by Guzzetti [9], considering the dynamical bifurcations and the changes in the stability of the motion along the family. With respect to the previous studies, the presence of the second order term of the gravity exerted on a finite dimension body slightly modifies the results of the current research work.

The previous results identify a strong connection between the size of the orbit and the associated periodic attitude motion, which is quite typical for this class of problems. Looking at the differences between the three

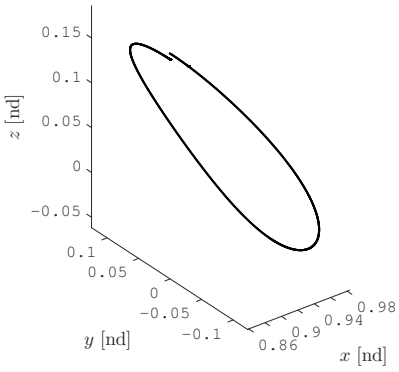


(a) Orbit Initial Guess

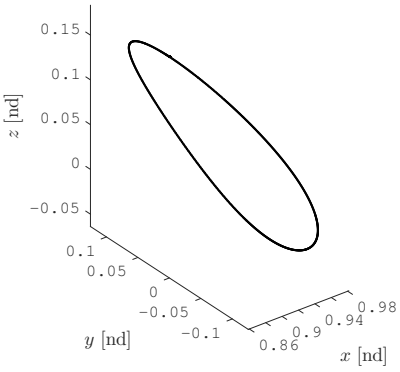


(b) Periodic Orbit

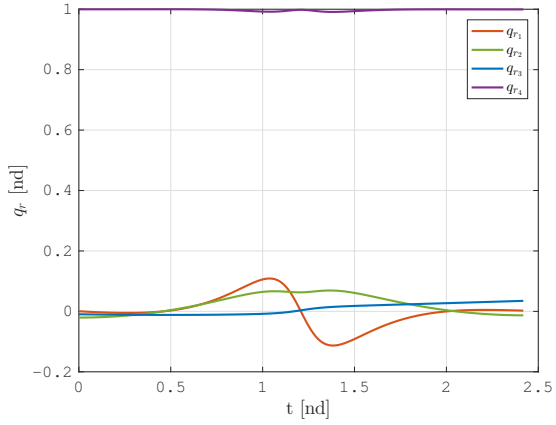


(c) Quaternions Initial Guess

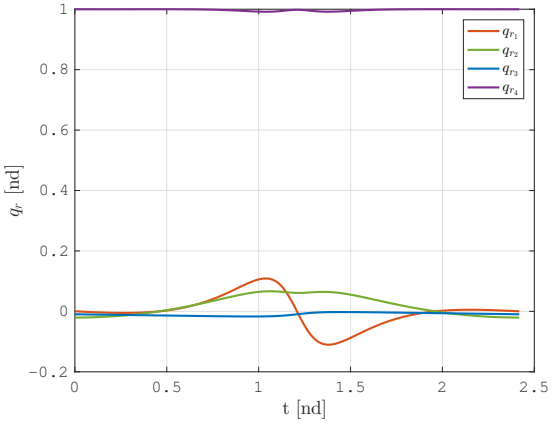


(d) Periodic Quaternions

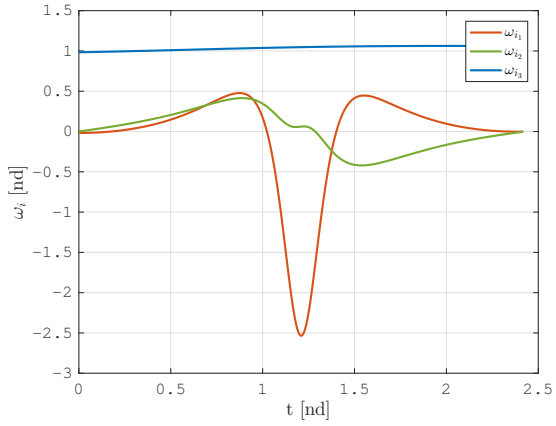


(e) Angular Velocity Initial Guess

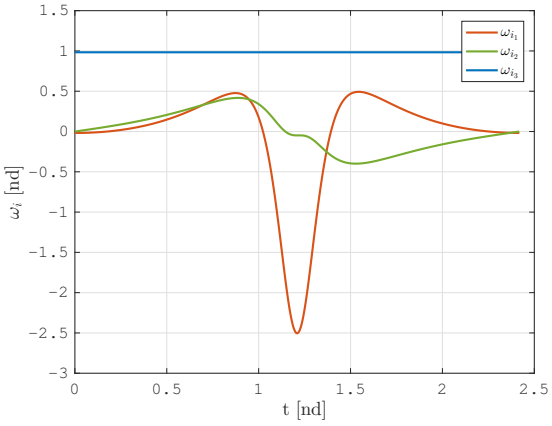


(f) Periodic Angular Velocity

Fig. 2: Initial Guess and Periodic Orbit-Attitude Dynamics. (EML1 Halo Orbit: $T_t = 10.5\,\mathrm{d}$ - $I_{max}/I_{min} = 1.5$).

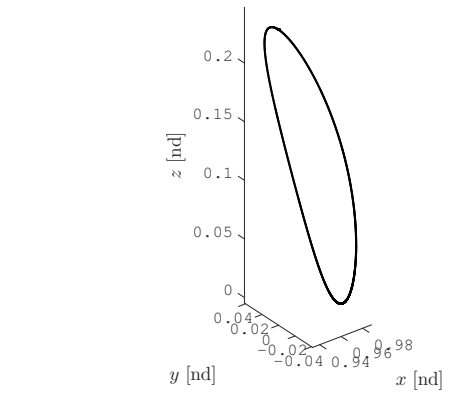


(a) Orbit

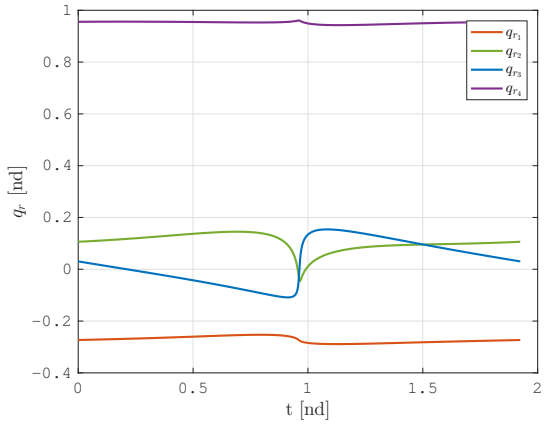


(b) Quaternions

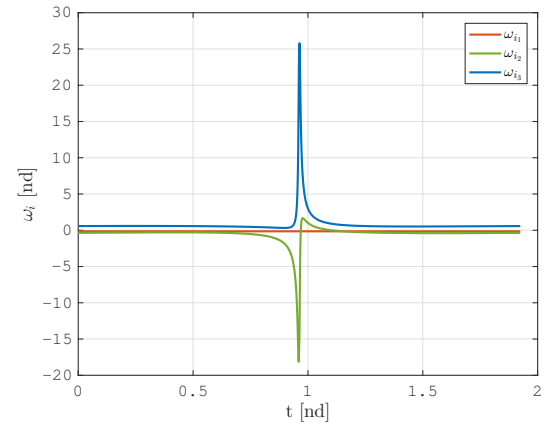


(c) Angular Velocity

Fig. 3: NRO Orbit-Attitude Periodic Dynamics. (EML1 NRO Orbit: $T_t = 8.5\,\mathrm{d}$ - $I_{max}/I_{min} = 1.5$).

different attitude families in figures 4b to 4d, it is evident that for a certain energy level of the orbital motion there exists a single family of attitude solutions. In fact, in the vicinity of each orbit shown in figure 4a, the allowed periodic rotational solutions share similar dynamical properties, such as the stability level or the quaternion subspace shape. Obviously, a minor change in the orbit would result in a small variation in the rotational motion. However, if the energy gap between two similar orbits is large enough to move across a bifurcation point, the attitude dynamics could have the features of distinct dynamical families. This example is representative of the coupling between orbital and attitude dynamics in non-Keplerian environment, but further investigation is warranted to understand the weight of this dynamical pairing.

An additional family of very important and useful planar orbits is the DRO family. DRO are remarkably stable in the long-term and can be reached at a reasonable cost. For these reasons, they may be exploited for many interesting applications around the Moon. An example of DRO family is reported in figure 5 for a rod like mass distribution with ratio between maximum and minimum inertia moments equal to 2.5. The different elements of the family share the same orbit, which has a period of $14\,\mathrm{d}$, but they differ for the number of overall rotations of $m$ in the synodic frame. In fact, the attitude dynamics in figure 5a shows 2 overall clockwise rotations in $S$, while figure 5b and figure 5d perform just one rotation per orbital period, respectively clockwise and counterclockwise. A particular scenario is represented by figure 5c, where the body is not spinning in $S$, but it is just librating about the equilibrium condition. Numerous periodic solutions of a single dynamical family with diverse spinning conditions open to a wide set of operational opportunities. In fact, the distinct attitude alternatives allow to exploit a single orbit, which may be constrained from several requirements coming from the mission design, for various operational phases. For example, the librating solution could facilitate the telecommunication subsystem, while the fast spinning one can be exploited to reduce the station-keeping effort, since a spinning platform behaves better, with respect to the librating configuration, in terms of perturbations counteracting.

## IV. Flexible Dynamics

At this point of the research, the rigid body dynamics assumption is discarded and the body $m$ is assumed to be flexible. Therefore, the effects of the previously shown dynamical evolutions on the structural dynamics of the space system have been studied. The outcomes of this investigation may be used to define the validity range in assuming rigid body motion while studying the dynamics of a large space structure in complex dynamical environments.

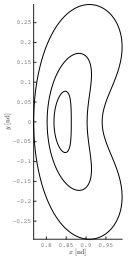

(a) Lyapunov Orbit

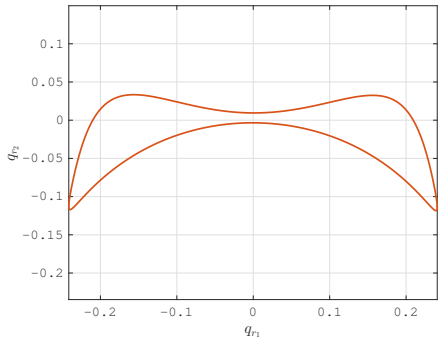


(b) Quaternions - Family 1

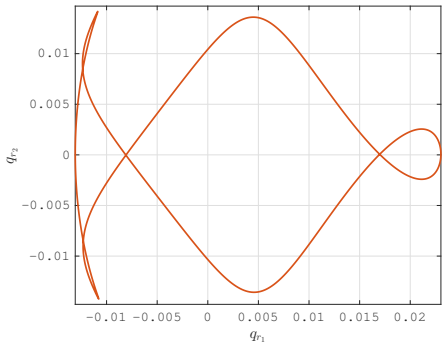


(c) Quaternions - Family 2

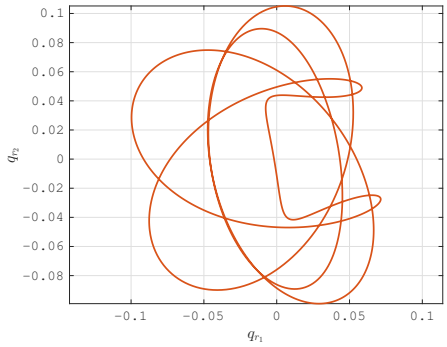


(d) Quaternions - Family 3

Fig. 4: Family of Lyapunov Orbit-Attitude Periodic Dynamics - Quaternion subspace, components 1 and 2. (EML1 Lyapunov Orbits: $T_{t_1} = 12.1\,\mathrm{d}$, $T_{t_2} = 14.1\,\mathrm{d}$ and $T_{t_3} = 18.88\,\mathrm{d}$ - $I_{max}/I_{min} = 5$).

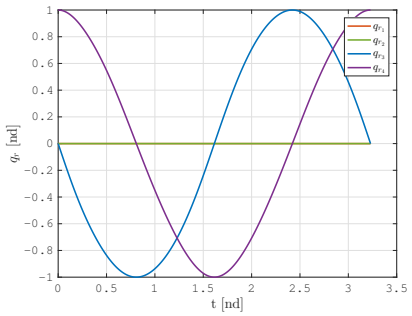


(a) 2 Rotations Clockwise

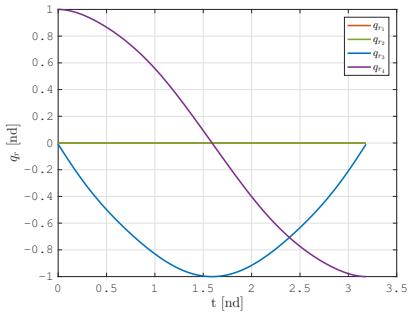


(b) 1 Rotation Clockwise

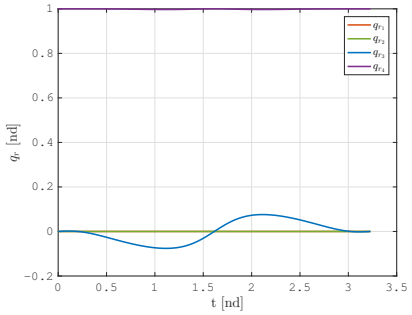


(c) Zero Spin

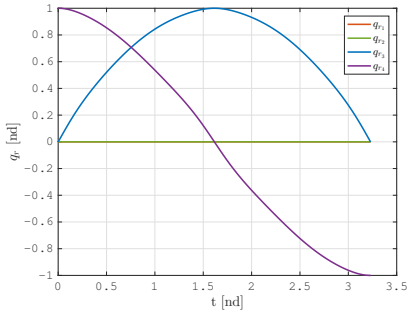


(d) 1 Rotation Counterclockwise

Fig. 5: Family of DRO Orbit-Attitude Periodic Dynamics, Different Spinning Velocities - Quaternions with respect to time. (EM DRO Orbit: $T_t = 14\,\mathrm{d}$ - $I_{max}/I_{min} = 2.5$).

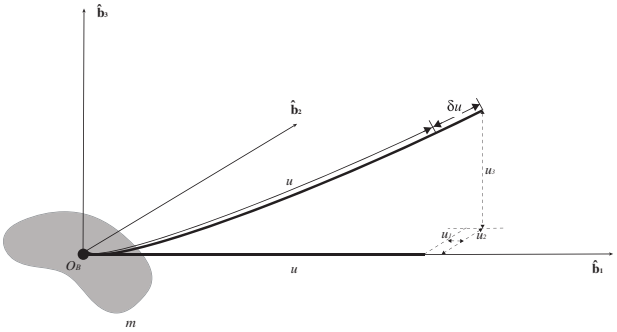


Fig. 6: Distributed Parameters Model (DPM).

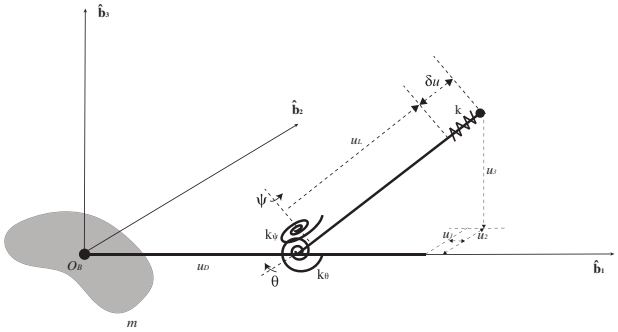


Fig. 7: Lumped Parameters Model (LPM).

This section is founded on the pioneering work of Kane, who studied the dynamics of flexible structure undergoing large overall motions [16]. In fact, a non-linear strain measure and a change of coordinates allow to automatically include numerous motion-induced effects, such as centrifugal stiffening or vibrations induced by Coriolis force, which are usually neglected by the canonical structural techniques based on linear Cartesian modelling approaches. A quadratic form of the strain energy helps to obtain an accurate model, which produces exact simulations and can be easily implemented for numerical computation through a Rayleigh-Ritz method to approximate the involved variables. The theoretical foundation of the developed model has been gathered from the work of Yoo [17] and other authors at the Aerospace Science and Technology Department of Politecnico di Milano [18]. The development of this work is a distributed parameters model of a flexible structure attached to the centre of mass of the body $m$ under the effects of the coupled orbit-attitude dynamics in CR3BP, displayed in figure 6 for the simple case of the cantilever beam. This model allows further extensions and different beams or plates may be attached to the same rigid body with minor modifications of the algorithm. All the non-linear strain terms due to the large motion of the flexible structure are retained, while the inertia forces are linearized to obtain the final equations of motion for the present modelling method, which can also be referred as foreshortening approach.

The distributed parameters technique is then exploited as a reference for a less refined but effective model, which is denoted in this paper as lumped parameters model. The lumped parameters model produces less precise results, but is less expensive in terms of computational load and allows an easier and faster investigation of space structures composed by many elements. In fact, both models for flexible dynamics have been developed exploiting a multi-body formulation and several simple elements can be interconnected to represent the structural dynamics of a complex spacecraft. However, if the overall structure is composed by numerous distributed parameter elements, the time to simulate a system is excessively long.

The lumped parameters technique, with reference to figure 7, is based on rigid rods, lumped masses and springs to represent the inertia and flexibility properties of a given extended flexible body. An algorithm has been developed to automatically write the analytical equations of motion of the system, once the list of the various elementary structural components and the mutual connection between them have been specified. The different elements are assembled exploiting rotation matrices between the local coordinate systems of each part of the structure and satisfying the imposed constraints. The resulting dynamic equations are obtained with a Lagrangian approach, starting from the Lagrangian function of the multi-body system.

The result reported in figure 8 shows a three-dimensional spin-up motion of a $10\,\mathrm{m}$ cantilever beam in free-space without any external force or torque. The beam is attached to a rigid base, with an angle of $45\mathrm{deg}$ with respect to the spinning axis of the support, which undergoes a prescribed spin-up motion characterized by the parameters stated in the caption of figure 8. Together with other simulations, the one discussed here has been used to validate the model with respect to the existing results of Yoo [17].

In figures 8 to 10 the dimensional units have been used in place of the non-dimensional ones, which are typically related with the CR3BP formulation. This change of units is due to the relationship of this part of the research with structural dynamics and its typical quantities. In fact, in this section the characteristic lengths are in the order of $10^1 - 10^2\ \mathrm{m}$ and the characteristic times in the order of $10^1\ \mathrm{s}$; hence, the use of non-dimensional units is not handy.

When the multi-body equations of motion are available, both for the distributed and the lumped parameters model, they are coupled with the periodic orbit-attitude dynamics transformed in the inertial non-rotating reference, and the

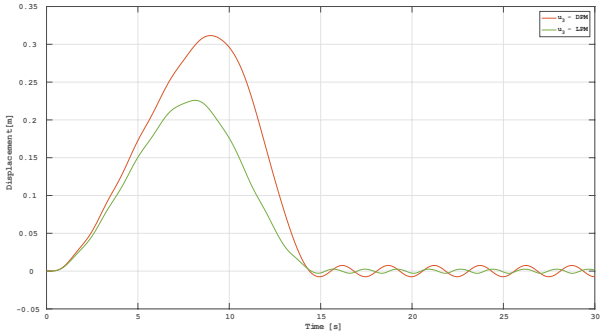


Fig. 8: Lumped and Distributed Parameters Model Validation. (Cantilever beam with $l_b = 10\,\mathrm{m}$, $m_b = 12\,\mathrm{kg}$ and elastic modulus $E_b = 71\,\mathrm{GPa}$. Spin-up motion: steady state angular speed $\Omega_s = 3\,\mathrm{rad/s}$ and time constant $T_s = 15\,\mathrm{s}$, as defined by Yoo [17]).

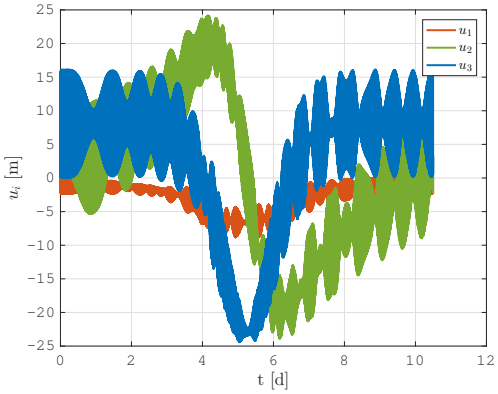


Fig. 9: Flexible Dynamics in Halo Orbit. (EML1 Halo Orbit: $T_t = 10.5\,\mathrm{d}$ - $I_{max}/I_{min} = 1.5$. Distributed Parameters Beam: $l_b = 100\,\mathrm{m}$, $\rho_b = 2800\,\mathrm{kg/m^3}$, $E_b = 71\,\mathrm{GPa}$ and first bending natural frequency $\phi_{b_1} = 0.06\,\mathrm{Hz}$).

flexible dynamics is propagated. However, the coupling is currently not full, since the effect of the flexible dynamics on the orbit-attitude motion is neglected in the present model. One example result is shown in figure 9, where the tip displacements of a distributed parameter beam aligned with the principal inertia axes of $m$ is plotted as a function of time. The coupled orbit-attitude dynamics that has been taken as input is related with a periodic solution similar to the one represented in figure 2. The displacements $u_1$, $u_2$ and $u_3$ are labelled according to figure 6. Note that the displacements are large when compared to real conditions, but they are due to the characteristics of the selected beam, which have been chosen to highlight the effects of flexibility. In fact, the beam is $100\,\mathrm{m}$ long, it has a square cross-section and it has the physical properties of a generic aerospace aluminium alloy ($\rho_{Al} = 2800\,\mathrm{kg/m^3}$ and $E_{Al} = 71\,\mathrm{GPa}$). The size of the cross-sectional area has been derived imposing a target first bending natural frequency in the order of the lowest frequency of the International Space Station, approximately equal to $0.06\,\mathrm{Hz}$. The flexible dynamics is therefore characterized by a quasi-static deformation due to the overall rotational motion, plus a superposition of the natural frequencies of the flexible structure. In fact, the dynamics in figure 9 is composed by a slow overall deformation and a fast sinusoidal oscillation with period of approximately $16\,\mathrm{s}$, corresponding to the first bending natural frequency. The resulting flexible behaviour is due to a complex interaction with the full orbit-attitude dynamics in the perturbed CR3BP.

The presented result is in agreement with other simulations that have been performed: a strong coupling between orbit-attitude dynamics and flexible dynamics seems to be not present. The flexibility properties of a space system may be selected independently from the planned orbit-attitude evolution. In fact, the dynamical response of the space structure is composed of a quasi-static term plus a superposition of natural modes, since there is a huge separation between typical lowest natural frequencies of real extended space systems and the one related with the non-Keplerian dynamics. This conclusion is valid in general also for other orbit-attitude periodic motions and extended structures with different physical properties, geometry and dimensions, as long as the natural frequencies of the extended structure stay well above the frequency content of the overall motion, which is true, in general, for actually feasible space systems. This statement can be explained looking at the frequency content of a periodic orbit-attitude dynamics; figure 10 shows a fast Fourier transform of the angular acceleration along a Halo orbit. Similar results are obtained considering various families of orbits and alternative dynamical quantities, such as the linear acceleration or the angular velocity.

## V. Large Space Structures in Halo Orbits

Research topics dealing with large space structures in cis-lunar space are of great interest in the scientific community of today, as explained in the first section of this paper. The present investigation has been carried out to have some preliminary insights on this modern and broad area of aerospace science.

The mutual influence of orbit-attitude and flexible dynamics should not be completely neglected, but seems to be reasonable to decouple the problem at least in the first

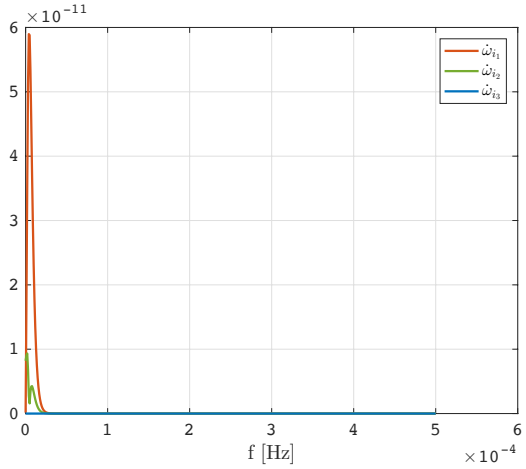


Fig. 10: Frequency Content of Angular Acceleration in Halo Orbit. (EML1 Halo Orbit: $T_t = 10.5\,\mathrm{d}$ - $I_{max}/I_{min} = 1.5$).

research phases. However, even if a rigid body is considered, different configurations and mechanical properties of the extended structure can have a strong effect on the coupled orbit-attitude dynamics. For instance, many periodic families are generated only by well-defined inertia parameters. For this reason, the study of the effect of dissimilar mass distribution on the periodic dynamics seems to be remarkably important. As example, the sequence in which a future space station will be assembled is of a maximum relevance. In that case, the inertia moments will vary in time, as docking operations are performed and independent modules are attached and detached from the main structure. These operations will have to be carefully planned to avoid the departure from a stable periodic dynamics or to minimize the station-keeping effort. Alternatively, particular operations may be designed in order to obtain unstable behaviours able to facilitate large manoeuvres and transfers.

Various simulations show that periodic solutions for large space structures in Halo orbits, both with regular amplitude or with large amplitude (NRO), have a lower orbit-attitude stability with respect to DRO. Small perturbations are able to arise deviations from the nominal attitude; thus active attitude control is needed. Moreover, the large angular acceleration corresponding to perilune passages might represent a potential issue for the structure of extended space structures.

## VI. Final Remarks

This paper was intended to present just few preliminary example results that may be obtained after some analyses with the developed models and algorithms. The information coming from the presented coupled orbit-attitude model may be used to drive the design of a large spacecraft in lunar vicinity. Additional information can be gathered from other analyses, hence a deeper investigation is needed and will follow this work.

The flexibility of a large space systems should not be neglected, but its influence seems to be not strongly coupled with the overall orbit-attitude dynamics. Further studies are needed in these regards, in particular if higher frequency phenomena are present and have to be inserted in the model. For instance, attitude dynamics associated with particular operational activities and manoeuvres or the presence of an active control system.

Also the importance of the coupling between orbital and attitude dynamics should be further investigated. In particular, dedicated analysis are needed to highlight the influence of the attitude motion on the dynamics of the centre of mass. The preliminary results discussed in this paper delineated a certain effect of the orbital dynamics on the associated naturally periodic rotational motion. A future research work will be directed to investigate more the magnitude of the orbit-attitude dynamics coupling, which has not been deepened in this paper because it was intended to study also the coupling with the flexible dynamics of the spacecraft.

The best orbit to host a large space structures in the vicinity of the Moon, together with the related coupled attitude dynamics, is far to be completely defined. However, this paper wants to underline the need to consider not only the orbital dynamics but also the rotational motion when dealing with large and flexible space structure in Halo and other classes of non-Keplerian orbits.

## References

[1] International Space Exploration Group (ISECG), "The global exploration roadmap", 2013.

[2] R. Whitley and R. Martinez, "Options for staging orbits in cis-lunar space", *NASA Technical Report*, 2015.

[3] T. R. Kane and E. Marsh, "Attitude stability of a symmetric satellite at the equilibrium points in the restricted three-body problem", *Celestial mechanics*, vol. 4, no. 1, pp. 78–90, 1971.

[4] W. Robinson, "Attitude stability of a rigid body placed at an equilibrium point in the restricted problem of three bodies", *Celestial Mechanics and Dynamical Astronomy*, vol. 10, no. 1, pp. 17–33, 1974.

[5] A. Abad, M. Arribas, and A. Elipe, "On the attitude of a spacecraft near a lagrangian point", *Bulletin of the Astronomical Institutes of Czechoslovakia*, vol. 40, pp. 302–307, 1989.

[6] E. Brucker and P. Gurfil, "Analysis of gravity-gradient-perturbed rotational dynamics at the collinear lagrange points", *The Journal of the Astronautical Sciences*, vol. 55, no. 3, pp. 271–291, 2007.

[7] B. Wong, R. Patil, and A. Misra, "Attitude dynamics of rigid bodies in the vicinity of the lagrangian points", *Journal of guidance, control, and dynamics*, vol. 31, no. 1, pp. 252–256, 2008.

[8] D. Guzzetti and K. C. Howell, "Coupled orbit-attitude dynamics in the three-body problem: A family of orbit-attitude periodic solutions", in *AIAA/AAS Astrodynamics Specialist Conference*, 2014.

[9] ——, "Natural periodic orbit-attitude behaviors for rigid bodies in three-body periodic orbits", *Acta Astronautica*, 2016.

[10] A. J. Knutson and K. C. Howell, "Application of kane's method to incorporate attitude dynamics into the circular restricted three-body problem", *AIAA/AAS Astrodynamics Specialist Conference*, 2012.

[11] A. J. Knutson, D. Guzzetti, K. C. Howell, and M. Lavagna, "Attitude responses in coupled orbit-attitude dynamical model in earth–moon lyapunov orbits", *Journal of Guidance, Control, and Dynamics*, vol. 38, no. 7, pp. 1264–1273, 2015.

[12] A. Colagrossi and M. Lavagna, "Dynamical analysis of rendezvous and docking with very large space infrastructures in non-keplerian orbits", *6th International Conference on Astrodynamics Tools and Techniques (ICATT)*, 2016.

[13] L. Bucci and M. Lavagna, "Coupled dynamics of large space structures in lagrangian points", *6th International Conference on Astrodynamics Tools and Techniques (ICATT)*, 2016.

[14] T. R. Kane, P. W. Likins, and D. A. Levinson, "Spacecraft dynamics", *New York, McGraw-Hill Book Co.*, vol. 1, 1983.

[15] W. S. Koon, M. W. Lo, J. E. Marsden, and S. D. Ross, "Dynamical systems, the three-body problem and space mission design", *Marsden Books*, 2008.

[16] T. R. Kane, R. Ryan, and A. Banerjee, "Dynamics of a cantilever beam attached to a moving base", *Journal of Guidance, Control, and Dynamics*, vol. 10, no. 2, pp. 139–151, 1987.

[17] H. Yoo, R. Ryan, and R. Scott, "Dynamics of flexible beams undergoing overall motions", *Journal of Sound and vibration*, vol. 181, no. 2, pp. 261–278, 1995.

[18] D. Invernizzi, "A foreshortening formulation for flexible structures undergoing large overall motions", *M.Sc. Thesis, Politecnico di Milano*, 2014.